Journal of Quantitative Spectroscopy & Radiative Transfer 203 (2017) 511–516

Contents lists available at ScienceDirect

Journal of Quantitative Spectroscopy & Radiative Transfer

journal homepage: www.elsevier.com/locate/jqsrt

Line list for the MgF ground state

Shilin Hou [a], Peter F. Bernath [b,*]

[a] Department of Physics, Ocean University of China, Qingdao, Shandong 266100, China
[b] Department of Chemistry and Biochemistry, Old Dominion University, Norfolk, Virginia 23529, USA

ARTICLE INFO

Article history:
Received 29 November 2016
Received in revised form
7 March 2017
Accepted 7 March 2017
Available online 11 March 2017

Keywords:
Molecular potential
Dipole moment function
Einstein A coefficient

ABSTRACT

An extended Morse oscillator (EMO) potential function was obtained by fitting the observed laboratory vibration-rotation and pure rotational spectra of the ^{24}MgF $X^2\Sigma^+$ ground state. The fitted potential reproduces the observed transitions within the observation uncertainties. With this EMO potential and an analytic dipole moment function in the form of a Padé approximant fitted using *ab initio* dipole moment data, line lists for ^{24}MgF, ^{25}MgF and ^{26}MgF were computed for $v \leq 8$, $N \leq 100$, $\Delta v = 0$–8. It was discovered that directly using the ab initio dipole moment points with cubic spline interpolation to calculate line intensities worked for $\Delta v < 3$, but failed for higher Δv values. A simple solution was found by fitting the ab initio dipole points with a suitable analytical dipole moment function. The calculated emission spectra are in good agreement with an observed laboratory spectrum with the MgF sample at 1823 K.

1. Introduction

The MgF molecule has been investigated extensively with different experimental and theoretical approaches [1–13]. A rotational analysis of the $A^2\Pi$-$X^2\Sigma^+$ electronic spectrum of MgF was performed by Barrow and Beale [1]; vibration-rotation lines for $v = 0$–7 and N up to 87 were analyzed by Barber *et al.* [2] from an infrared emission spectrum; millimeter-wave transitions were observed by absorption spectroscopy by Anderson *et al.* [3,4] for $v = 0$–3, N from 2 to 12.

MgF is a potential astrophysical molecule [4,5]. Metal salts such as NaCl, AlCl and KCl have been detected in the circumstellar shell of the cool carbon star IRC+10216 [14]. The identification of magnesium compounds in IRC+10216 [15,16] demonstrated that there is enough magnesium in the gas phase to form simple molecules. The observation of AlF [5] in the same object suggests that other metal fluorides may be present as well. Thus, it is possible that MgF may be detectable in objects such as IRC+10216, particularly with millimeter arrays such as SMA and ALMA, which led to the detection of TiO and TiO_2 in VY Canis Majoris [17]. MgO is also predicted to be present in the atmospheres of hot rocky super-Earth exoplanets [18] and MgF might also be present.

As an ionic free radical, MgF molecule is also of particular theoretical interest. Various *ab initio* calculations show that the molecule is very ionic near equilibrium, but as the bond distance increases there is a curve crossing and MgF is covalent at long range near dissociation [7–13]. The electron spin resonance measurements by Knight *et al.* [6] showed that the spin density on the F atom is less than 4%, which supports the ionic picture of the radical as Mg^+F^-. The unpaired electron is located almost exclusively on the metal atom. Very recently, it has been suggested that laser cooling and magneto-optical trapping of MgF is possible [13] using the $A^2\Pi$-$X^2\Sigma^+$ transition.

The goal of the present work is to provide a MgF line list for the quantitative analysis and prediction of infrared spectra of hot MgF as found for example in exoplanets. The ro-vibrational line positions (and line intensities) are obtained by direct solution of the nuclear motion Schrödinger equation using Le Roy's computer program LEVEL [19] with an accurate empirical potential energy function. The potential energy function was obtained by fitting the pure rotation [3,4] and vibration-rotation [2] data using LeRoy's dPotFit code [20]. The potential function used was an Expanded Morse Oscillator (EMO) [21] similar to the work of Barton et al. [22] on NaCl and KCl.

The ground state potential energy function was studied with both *ab initio* and empirical approaches. The *ab initio* data were obtained to study the behavior over the full range the potential; the empirical potential was used to improve the accuracy of the predicted vibration-rotation transitions. All *ab initio* computations were performed with the Molpro2012 [23] package.

An experimental dipole moment is not available for MgF so had to be obtained from *ab initio* calculations. The calculated line intensities are very sensitive to the form of the dipole moment function and its derivatives [24]. Dipole moment functions from several different *ab initio* approaches were therefore tried

* Corresponding author.
E-mail address: pbernath@odu.edu (P.F. Bernath).

http://dx.doi.org/10.1016/j.jqsrt.2017.03.019
0022-4073/

including the MRCI [25,26] (multireference configuration interaction method) and the ACPF (averaged coupled-pair functional) methods [27,28]. The calculated dipole moment points were fitted by least squares to a Padé approximant, which was then used in the LEVEL program to calculate the line intensities.

2. EMO potential function

As for NaCl [22], the observed MgF line positions are reproduced using Le Roy's EMO potential model [21], which can be expressed as

$$V(r) = D_e[1-e^{-\phi(r)(r-r_e)}]^2 \quad (1)$$

where

$$\phi(r) = \sum_{i=0}^{N} \beta_i y_p(r, r_e)^i \quad (2)$$

$$y_p(r, r_e) = \frac{r^p - r_e^p}{r^p + r_e^p}. \quad (3)$$

D_e is the potential well depth and r_e is the equilibrium distance. N (=6) and p (=3) are preset parameters, and β_i are parameters determined using Le Roy's dPotFit code [20]. D_e was fixed to a literature value and r_e was determined by the fit. The observed transitions used in the fit are summarized in Table 1.

D_e was set to 37297.24 cm^{-1}, which was obtained using $D_e = D_0 + E_0$, with D_0 taken from Haynes [29], and the zero-point energy E_0 calculated from the spectroscopic constants of Barber *et al.* [2]. In total 763 observed transitions were fitted with a dimensionless standard error (DSE) of 1.026. The ^{24}MgF pure rotation data were corrected for the effects of fine and hyperfine structure as in Barber et al. [2]. For the vibration-rotation lines, the uncertainties assigned in the original experimental work [2], in the range of 0.001 cm^{-1} – 0.005 cm^{-1}, were used and for the millimeter-wave data [3,4], an uncertainty of 9.3×10^{-7} cm^{-1} was adopted. These uncertainties correspond to one standard deviation. The small spin splitting and F hyperfine structure was not resolved in the vibration-rotation spectrum recorded at 0.01 cm^{-1} [2] resolution and MgF was treated as if the ground state has $^1\Sigma^+$ symmetry. In the present work we aim to provide a vibration-rotation line list so we follow Barber et al. [2] and ignore fine and hyperfine structure. The EMO potential parameters obtained from dPotFit are presented in Table 2 along with 95% confidence limits.

3. *Ab initio* potential and dipole moment function

3.1. ACPF potential and dipole moment

We found that the averaged coupled-pair functional (ACPF) approach [26,27] with the correlation-consistent polarized valence 5-zeta (cc-pV5Z) basis set of Dunning and co-workers [30–33] gives a reliable potential with satisfactory parameters at the equilibrium bond length. The complete active space multi-configurational self-consistent field (CASSCF) [34,35] wave function with the same electron configuration was taken as the reference in this ACPF calculation. All the core orbitals were frozen, and the active space of 14 orbitals ($8a_1$,$3b_1$,$3b_2$) was used for 9 valence electrons in the calculations. A considerable number of trial calculations were carried out with basis sets that ranged from vdz (cc-pvdz) to av5z (aug-cc-pv5z) for Mg and from vdz to av6z for F for both ACPF and MRCI (multi-reference configuration interaction) methods although not all calculations were successful. The ACPF/cc-pV5Z calculation was selected based on the values of r_e, ω_e and the shape of the dipole moment function.

The r_e from our ACPF calculation is 1.7452 Å which was in excellent agreement with the experimental value, r_e = 1.7499 Å [2]. The calculated dipole moment (3.004 D) at r_e from ACPF is close to literature [8–12] values (2.86–3.13 D) from different *ab initio* methods, which are listed in Table 3. We note our ACPF dipole moment is from an optimization computation, which is slightly different than the value obtained by a single point calculation at the experimental r_e.

The ACPF potential curve is smooth and agrees well with the EMO curve over most of the potential well as shown in Fig. 1. The *ab initio* points differ from the EMO potential from about 3 Å to 5 Å, which is far from the range of the observed data (< 6000 cm^{-1} from the minimum). Fig. 1 suggests that the EMO potential may be reliable up to about 20000 cm^{-1} from the bottom of the potential well. Therefore, some transitions slightly above the observed data range can be reliably predicted from this EMO potential. At long range, the EMO potential is not satisfactory, but this is out of the scope of the present research.

The shape of the ACPF dipole moment function is smooth in the

Table 2
EMO potential parameters for MgF ground state.

	MgF EMO(N=6, p=3)	Uncertainty
D_e/cm^{-1}	37297.24	Fixed
r_e/Å	1.749929860871D+00	1.2D-07
β_0	1.478548128092D+00	1.4D-06
β_1	−2.525625987692D-01	3.0D-05
β_2	1.071472042379D-01	1.3D-04
β_3	4.191108679134D-02	2.0D-03
β_4	9.576638726358D-02	4.3D-03
β_5	1.125082555037D-01	4.0D-02
β_6	1.617929283898D-01	9.7D-02

Table 3
Dipole moment for the MgF ground state at r_e from various calculations.

Methods	Dipole moment	Reference	
FD-HF	3.1005 D	Kobus, *et al.*	[10]
MHF	3.1005 D	Kobus, *et al.*	[10]
SCF	3.098 D	Langhoff *et al.*	[12]
SDCI	3.048 D	Langhoff *et al.*	[12]
CPF	3.077 D	Langhoff *et al.*	[12]
CASSCF	2.8611 D	Fowler & Sadlej 1991	[11]
MRCI+Q	3.126 D	Wu *et al.*	[9]
ACPF	3.004 D	This work[a]	

[a] Optimization result, which is slightly different than the single point calculation at the experimental r_e.

Table 1
Laboratory data used to determine the MgF potential energy curve.

MgF	Transitions	Wavenumber range	Uncertainty
Anderson,et al. [3,4]	$\Delta\upsilon=0$, $\Delta N=+1$ $\upsilon=0$–3, $N \le 12$	3.1–12.3 cm^{-1}	9.3×10^{-7} cm^{-1}
Barber,et al. [2]	$\Delta\upsilon=1$, $\Delta N=\pm 1$ $\upsilon=0$–7, $N \le 87$	580–762 cm^{-1}	0.001–0.005 cm^{-1}

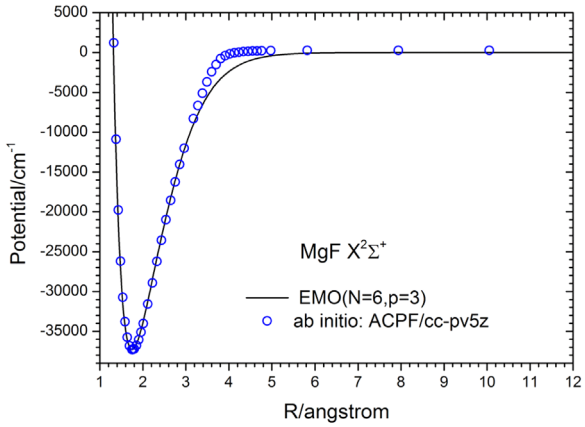

Fig. 1. EMO and ACPF potential for MgF ground state.

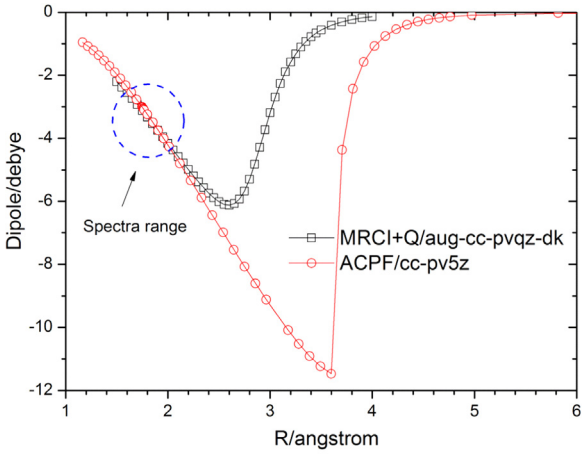

Fig. 2. *Ab initio* dipole moment functions for MgF ground state. The MRCI+Q data are taken from Ref. [9].

range of the spectroscopic data and has a maximum absolute value at larger r before returning to zero at long range (Fig. 2). For comparison, Fig. 2 includes values from an MRCI+Q calculation from the literature [9]. The ACPF dipole moment shows an abrupt change at $r \approx 3.6$ Å, while the MRCI+Q curve is smoother. This type of variation with r is characteristic of ionic molecules which dissociate to neutral fragments. Near equilibrium the dipole moment function is approximately linear but at large internuclear separation there is a curve crossing with at least one potential energy function in which the charge separation is small (i.e., the character of the ground state wavefunction changes rapidly from Mg^+F^- to MgF). Based on the electronegativity of F and the first ionization potential of Mg [29], this curve crossing occurs near 3.39 Å.

For MgF the change from ionic to covalent bonding happens outside the data range so should not affect our calculation of the line intensities. Indeed, both dipole moment functions shown in Fig. 2 give very similar intensities for the observed lines. However, when the dipole moment points from the ACPF or the MRCI+Q calculations are used directly in the LEVEL program using the built-in cubic spline interpolation, the overtone transition intensities were unphysical for $\Delta v \geq 3$. To solve this problem different approaches were tested, including improving the numerical accuracy of LEVEL by using quadruple precision for the variables. In the end, we found that using an analytical form to represent the dipole moment data is a simple solution.

Table 4
Fitted Padé approximant coefficients M_0 and a_i (i=1–7) for the MRCI+Q dipole moment.

M_0 /a_i (i=1–7)	Values
M_0	−1.230 a.u. (Fixed ~3.126 D)
a_1	0.814292898376826
a_2	−0.317695561202887
a_3	0.490123252940770
a_4	31.2269237848287
a_5	−104.976868847063
a_6	96.1926230543182
a_7	20.4211738988439

3.2. Padé approximant representation of the dipole moment

Following the work on hydrogen halide ground states by Li *et al.* [24] we take the dipole moment function in the form of a Padé approximant as:

$$M(x) = M_0 \frac{(1+x)^3}{1+\sum_{i=1}^{7} a_i x^i} \quad (4)$$

in which $x=(r-r_e)/r_e$, M_0 is the dipole moment at r_e, and a_i are the fitting coefficients. This functional form has the correct r^3 limiting behavior at small r and r^{-4} for large r [36,37]. For the literature MRCI+Q/aug-cc-pVQZ-dk dipole moment [9], the M_0 value was set to 1.23 a.u. (3.126 D), which corresponds to the experimental r_e (1.7499 Å), not the MRCI+Q calculated r_e (1.7640 Å). The corresponding a_i coefficients obtained from the least squares fit are listed in Table 4. Note the MRCI+Q D_e (~37827 cm^{-1}) and the potential curve are similar to our ACPF results. The RMS (root mean square) of the fit using all of the MRCI+Q data (1.5 Å to 4 Å) is 3.6E-3 a.u. The obtained analytical function (Eq. (4)) and the literature dipole moment points are plotted in Fig. 3. The dipole moment points from both the ACPF and the MRCI+Q calculations are provided as supplementary data files (S1 and S2). The analytic dipole moment function is smooth and has good behavior at both $r=0$ and $r=\infty$; therefore, it is a physically acceptable function for intensity calculations for MgF. For the ACPF points, it was difficult to obtain a satisfactory simple analytical dipole moment function. Therefore, only the Padé representation of the MRCI+Q dipole moment data was used in the final line list calculation with the EMO potential. The transition dipole moments (TDMs) from this Padé function are compared in Fig. 4 with the results directly obtained with the *ab initio* dipole moment points of the ACPF and MRCI+Q calculations.

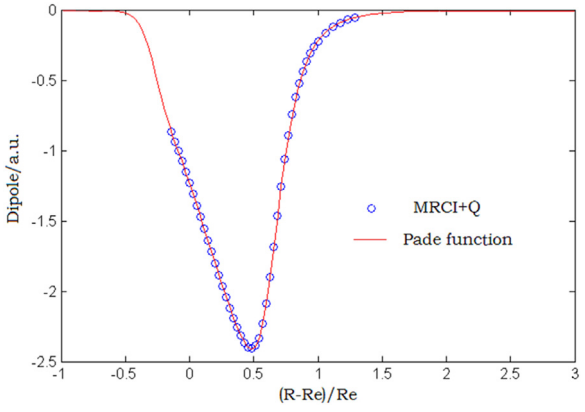

Fig. 3. Fitted Padé function for MgF dipole moment with the MRCI+Q data from Ref.[9]. The coefficients are given in Table 4.

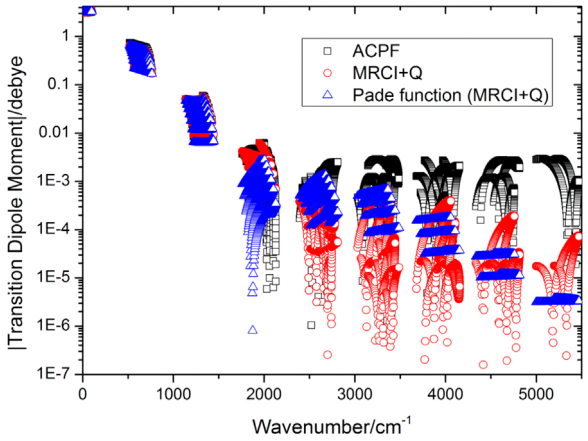

Fig. 4. Distribution of the TDMs calculated using different dipole moment functions. Notice that the $\Delta v=3$ (near 2000 cm^{-1}) TDMs are anomalously weak and there is a strong rotational dependence.

4. Line list

Although MgF has a $^2\Sigma^+$ ground state, the spin-rotation splitting is small and is not observed in the vibration-rotation emission spectrum [2]. MgF was therefore treated as a $^1\Sigma^+$ state [2] for the purposes of generating vibration-rotation line lists. Using the EMO potential for ^{24}MgF and the Padé form of the MRCI+Q dipole moment [9], ro-vibrational line lists (Supplementary tables S3, S4, S5) were obtained for ^{24}MgF, ^{25}MgF, and ^{26}MgF with Le Roy's LEVEL program [18].

As expected, LEVEL produces transitions nearly identical to those from dPotFit for ^{24}MgF. LEVEL also produces transition dipole matrix elements, the corresponding Einstein A values for each line and a set of band constants (B_v, D_v, H_v, …, O_v) for each vibrational level (Table S6, supplementary). These band constants are useful for simulating spectra with a program such as PGOPHER [38]. Line lists for all possible allowed transitions with $v=0$–8, $N \leq 100$, with $\Delta N = \pm 1$, are calculated for the ^{24}MgF, ^{25}MgF, and ^{26}MgF isotopologues and available as supplementary files (S3, S4 and S5). Born-Oppenheimer breakdown effects were ignored in the line list calculations since Mg and F are relatively heavy nuclei. For most of the observed ro-vibrational transitions of ^{24}MgF, the differences between the calculated and the observed transitions from Barber *et al.* [2] are less than 0.005 cm^{-1}.

The calculated emission line intensities, *I*, for ^{24}MgF (at 1823 K) are presented in Fig. 5 as an overview and in Fig. 6 for a short segment of the observed spectrum [2]. These intensities (in units of s^{-1}/molecule) are estimated as relative photon emission rates [39]:

$$I = A\left[\frac{g_{upper}}{Q} e^{\frac{-E_{upper}}{kT}}\right], \quad (5)$$

in which *Q* is the partition function, *A* is the Einstein *A* coefficient (s^{-1}) and g_{upper} is the upper state degeneracy. As expected, the strongest spectra appear in the 600–800 cm^{-1} range, corresponding to the $\Delta v=1$ transitions. For the overtone bands, the intensities for $\Delta v=3$ and, to a lesser extent, $\Delta v=4$ are anomalously low, but the overall pattern of band intensities is reasonable. Presumably the specific shape of the dipole moment function of MgF is responsible for the deviations from the typical decrease in intensity of about a factor of 10 for each increase in Δv [40].

As a test of our line lists we simulated the emission spectrum of ^{24}MgF using PGOPHER for comparison with the observed spectrum of Barber *et al.* [2] recorded with a sample temperature of 1823 K. The positions and relative intensities agree well as presented in Fig. 6.

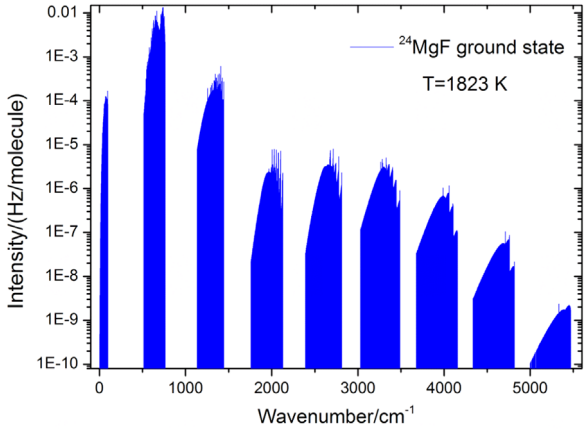

Fig. 5. Calculated overall emission intensity distribution for ^{24}MgF transitions in the range of $v \leq 8$, $N \leq 100$, $\Delta v=0$–8, and $\Delta N = \pm 1$, at 1823 K. Dipole moment function uses the fitted Padé approximant Eq.(4) with the MRCI+Q data from Ref. [9].

5. Discussion of overtone intensities

In our initial work, we calculated the line intensities using the ACPF/cc-pv5z dipole moment points directly in LEVEL with cubic spline interpolation. We noted that line intensities of $\Delta v=3$ overtone bands were weak and the intensities increased slightly with Δv for $\Delta v=4$–7 (Fig. 4). This increase is unphysical. We then tried the dipole moment points from an MRCI+Q/aug-cc-pVQZ-dk calculation [9], and some improvement was noted (Fig. 4). LEVEL was also converted from using Double Precision variables to Quadruple Precision, but there was little effect except for very high Δv values outside the range of interest. Finally, by fitting the MRCI+Q dipole moment points with an analytical function, Eq. (4), a more reasonable intensity distribution was obtained (Fig. 4). Very recently a similar effect and a similar solution using analytical dipole moment functions was described by Medvedev et al. [40] for CO overtones.

The intensity of a line as measured by the Einstein *A* value is given by the expression [19,39]:

$$A = 3.1361889\times10^{-7}\frac{S(J',J'')}{2J'+1}\nu^3\left|\left\langle\Psi_{v'J'}|M(r)|\Psi_{v''J''}\right\rangle\right|^2 \quad (6)$$

in which *A* is in s^{-1} units, M(*r*) is the dipole moment function in debye, ν the transition frequency in cm^{-1}, S(J'J") is a Hönl-London rotational factor, and $\Psi_{v'J'}$ and $\Psi_{v''J''}$ are the vibrational wave functions (which depend on *J* from the centrifugal potential). From Eq. (6), the two main factors that influence the transition intensities between two states in a given electronic state are the wave function Ψ_{vJ} and the dipole moment function *M*(r). The vibrational wave function Ψ_{vJ} and the transition frequencies ν are determined by the effective molecular potential function $V_{eff}(r)=V+V_{cent}$ [39], which in this work uses an accurate fitted EMO potential function for *V*. In our case, the main factor that influences the calculated intensities is therefore the dipole moment function *M*(r). For fundamental transitions, both the present ACPF and the literature [9] MRCI+Q points produce similar relative intensities compared to the observed spectrum [2] of ^{24}MgF. For overtone transitions, however, there can be numerical problems associated with interpolation of discrete points that contain small amounts of "noise" (i.e., *ab initio* points are not in fact "smooth", for example, because of the convergence criteria used). Using an analytical form to represent the *ab initio* dipole data is a simple solution [40]. The Padé approximant [24,36,37], Eq. (4), used in this work not only fits all the high quality MRCI+Q *ab initio* dipole points well, but also extrapolates properly to R=0 and R=∞.

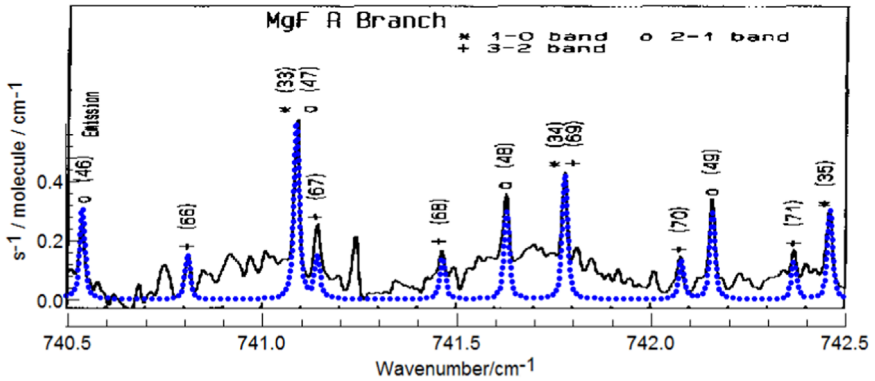

Fig. 6. Comparison of the observed and calculated MgF emission spectrum for part of the R-branch at 1823 K. Experimental spectrum (solid; black) is from Barber *et al.* [2]. Simulated line profiles (blue dotted line) were obtained with PGOPHER [37].

6. Conclusion

Line lists are calculated for the ground state MgF isotopologues with an accurate empirical potential function which reproduces the observed transitions within experimental uncertainty. The intensities of the transitions are predicted with high level *ab initio* ACPF/cc-pv5z and MRCI+Q/aug-cc-pvqz-dk dipole moment data. For overtone transitions, an analytical representation of the *ab initio* dipole moment function gives a more reliable estimate of line intensities. In particular, a Padé approximant based on the MRCI+Q/aug-cc-pvqz-dk dipole moment points is used to calculate the line intensities. All transitions for $v<9$, $\Delta v=0$–8, $\Delta N=\pm 1$, $N\leq 100$ were predicted for ^{24}MgF, ^{25}MgF, and ^{26}MgF.

Acknowledgements

This work is supported by China Scholarship Council, Shandong Province Natural Science Foundation (ZR2015AM009). Some support to PFB was provided by the NASA Origins of Solar Systems program. We thank D.-I. Wu for providing us with the dipole moment points from his ab initio calculations, J. Brooke for help with PGOPHER and R. J. Le Roy for helpful discussions.

Appendix A. Supporting information

Supplementary data associated with this article can be found in the online version at http://dx.doi.org/10.1016/j.jqsrt.2017.03.019.

References

[1] Barrow RF, Beale JR. Rotational analysis of electronic bands of gaseous MgF. Proc Phys Soc 1967;91:483–488.
[2] Barber BE, Zhang KQ, Guo B, Bernath PF. Vibration-rotation emission spectrum of MgF. J Mol Spectrosc 1995;169:583–589.
[3] Anderson MA, Allen MD, Ziurys LM. Millimeter-wave spectroscopy of MgF: structure and bonding in alkaline–earth monofluoride radicals. J Chem Phys 1994;100(2):824–830.
[4] Anderson MA, Allen MD, Ziurys LM. Millimeter and sub-millimeter rest frequencies for the MgF radical. Astrophys J 1994;425:L53–L57.
[5] Ziurys LM, Apponi AJ, Phillips TG. Exotic fluoride molecules in IRC+10216: confirmation of AlF and searches for MgF and CaF. Astrophys J 1994;433(2):729–732.
[6] Knight Jr LB, Easley WC, Weltner Jr W, Wilson M. Hyperfine interaction and chemical bonding in MgF, CaF, SrF, and BaF molecules. J Chem Phys 1971;54:322–329.
[7] Buckingham AD, Olegario RM. Hyperfine coupling in alkaline earth monofluorides. Limitations of the ionic model. Chem Phys Lett 1993;212(3-4):253–259.
[8] Pelegrini M, Vivacqua CS, Roberto-Neto O, Ornellas FR, Machado FBC. Radiative transition probabilities and lifetimes for the band systems $A^2\Pi-X^2\Sigma^+$ of the isovalent molecules BeF, MgF and CaF. Braz J Phys 2005;35:950–956.
[9] Wu DL, Tan B, Qin JY, Wan HJ, Xie AD, Yan B, Ding DJ. Ab initio calculations on potential energy curves and radiative lifetimes for the band systems $A^2\Pi-X^2\Sigma^+$ of magnesium monohalides MgX (X = F, Cl, Br, I). Spectrochim Acta A 2015;150:499–503.
[10] Kobus J, Moncrieff D, Wilson S. Comparison of the electric moments obtained from finite basis set and finite-difference Hartree-Fock calculations for diatomic molecules. Phys Rev A 2000;62:062503.
[11] Fowler PW, Sadlej AJ. Correlated studies of electric properties of ionic molecules: alkali and alkaline-earth hydrides, halides and chalcogenides. Mol Phys 1991;73:43–55.
[12] Langhoff SR, Bauschlicher Jr CW, Partridge H, Ahlrichs R. Theoretical study of the dipole moments of selected alkaline-earth halides. J Chem Phys 1986;84:5025–5031.
[13] Xu L, Yin Y, Wei B, Xia Y, Yin J. Calculation of vibrational branching ratios and hyperfine structure of $^{24}Mg^{19}F$ and its suitability for laser cooling and magneto-optical trapping. Phys Rev A 2016;93:013408.
[14] Cernicharo J, Guélin M. Metals in IRC+10216-Detection of NaCl, AlCl, and KCl, and tentative detection of AlF. Astron Astrophys 1987;183:L10–L12.
[15] Cabezas C, Agúndez M, Mata S, Guélin M, Peña I. Laboratory and Astronomical Discovery of Hydromagnesium Isocyanide. Astrophys J 2013;775:133.
[16] Kawaguchi K, Kagi E, Hirano T, Takano S, Saito S. Laboratory spectroscopy of MgNC–the first radioastronomical identification of Mg-bearing molecule. Astrophys J 1993;406:L39–L42.
[17] Kamiński T, Gottlieb CA, Menten KM, Patel NA, Young KH, Brünken S, et al. Pure rotational spectra of TiO and TiO_2 in VY Canis Majoris. Astron Astrophys 2013;551:A113.
[18] Schaefer L, Lodders K, Fegley Jr B. Vaporization of the earth: application to exoplanet atmospheres. Astrophys J 2012;755:41.
[19] Le Roy RJ. LEVEL: a computer program for solving the radial Schrödinger equation for bound and quasibound levels. J Quant Spectrosc Rad Transf 2017;186:167–178.
[20] Le Roy RJ. dPotFit: a computer program to fit diatomic molecule spectral data to potential energy functions. J Quant Spectrosc Rad Transf 2017;186:179–196.
[21] Le Roy RJ. Determining Equilibrium Structures and Potential Energy Functions for Diatomic Molecules. In: Demaison J, Csaszar AG, editors. Ch. 6, 159-203 in Equilibrium Structures of Molecules. London: Taylor and Francis; 2011.
[22] Barton EJ, Chui C, Golpayegani S, Yurchenko SN, Tennyson J, Frohman DJ, Bernath PF. ExoMol molecular line lists V: the ro-vibrational spectra of NaCl and KCl. Mon Not R Astron Soc 2014;442(2):1821–1829.
[23] MOLPRO version.1 is a package of ab initio programs written by Werner H-J, Knowles PJ, Knizia G, Manby FR, Schütz M, Celani P, Korona T, Lindh R, Mitrushenkov A, Rauhut G, Shamasundar KR, Adler TB, Amos RD, Bernhardsson A, Berning A, Cooper DL, Deegan MJO, Dobbyn AJ, Eckert F, Goll E, Hampel C, Hesselmann A, Hetzer G, Hrenar T, Jansen G, Köppl C, Liu Y, Lloyd AW, Mata RA, May AJ, McNicholas SJ, Meyer W, Mura ME, Nicklass A, O'Neill DP, Palmieri P, Peng D, Pflüger K, Pitzer R, Reiher M, Shiozaki T, Stoll H, Stone AJ, Tarroni R, Thorsteinsson T, Wang M. See ⟨http://www.molpro.net⟩; 2012.
[24] Li G, Gordon IE, LeRoy RJ, Hajigeorgiou PG, Coxon JA, Bernath PF, Rothman LS. Reference spectroscopic data for hydrogen halides. Part I: construction and validation of the ro-vibrational dipole moment functions. J Quant Spectrosc Rad Transf 2013;121:78–90.
[25] Werner H-J, Knowles PJ. An efficient internally contracted multiconfiguration-reference configuration interaction method. J Chem Phys 1988;89:5803–5814.
[26] Knowles PJ, Werner H-J. An efficient method for the evaluation of coupling coefficients in configuration interaction calculations. Chem Phys Lett 1988;145:514–522.
[27] Gdanitz RJ, Ahlrichs R. The averaged coupled-pair functional (ACPF): a size-extensive modification of MRCI(SD). Chem Phys Lett 1988;143:413–420.
[28] Shamasundar KR, Knizia G, Werner H-J. A new internally contracted multi-reference configuration interaction method. J Chem Phys 2011;135:054101.
[29] Haynes WM, editor. CRC Handbook of Chemistry and Physics. 95th edition. Boca Raton, FL.: CRC press; 2014.
[30] Dunning TH. Gaussian basis sets for use in correlated molecular calculations. I. The atoms boron through neon and hydrogen. J Chem Phys 1989;90:1007–1023.

[31] Kendall RA, Dunning Jr TH, Harrison RJ. Electron affinities of the first-row atoms revisited. Systematic basis sets and wave functions. J Chem Phys 1992;96:6796–6806.
[32] Woon DE, Dunning Jr TH. Gaussian basis sets for use in correlated molecular calculations. V. Core-valence basis sets for boron through neon. J Chem Phys 1995;103:4572–4585.
[33] Wilson AK, van Mourik T, Dunning Jr TH. Gaussian basis sets for use in correlated molecular calculations. VI. Sextuple zeta correlation consistent basis sets for boron through neon. J Mol Struct: THEOCHEM 1996;388:339–349.
[34] Werner H-J, Knowles PJ. A second order multiconfiguration SCF procedure with optimum convergence. J Chem Phys 1985;82:5053–5063.
[35] Knowles PJ, Werner H-J. An efficient second-order MC SCF method for long configuration expansions. Chem Phys Lett 1985;115(3):259–267.
[36] Ogilvie JF, Rodwell WR, Tipping RH. Dipole moment functions of the hydrogen halides. J Chem Phys 1980;73:5221–5229.
[37] Goodisman J. Dipole-Moment Function for Diatomic Molecules. J Chem Phys 1963;38:2597–2599.
[38] Western CM. PGOPHER: a program for simulating rotational, vibrational and electronic spectra. J Quant Spectrosc Rad Transf 2017;186:221–242.
[39] Bernath PF. Spectra of Atoms and Molecules. 3rd edition. New York: Oxford University Press; 2016.
[40] Medvedev ES, Meshkov VV, Stolyarov AV, Ushakov VG, Gordon IE. Impact of the dipole-moment representation on the intensity of high overtones. J Mol Spectrosc 2016;330:36–42.